New measurement of the critical exponent β for nickel by microwave transmission*

J. David Cohen† and Thomas R. Carver
Joseph Henry Laboratories, Princeton University, Princeton, New Jersey 08540
(Received 16 August 1976)

We measure the critical exponent β for spontaneous magnetization in thin foils of polycrystalline and single-crystal nickel, with results, $\beta = 0.357 \pm 0.008$ for a reduced temperature range of $10^{-2} < \epsilon < 10^{-1}$ and 0.358 ± 0.003 for a reduced temperature of $5 \times 10^{-3} < \epsilon < 10^{-1}$, respectively. These values lie significantly lower than values obtained by such nuclear hyperfine probe methods as angular correlation and Mössbauer absorption, and somewhat larger than values obtained by applied-field methods extrapolated to zero or NMR methods. Since this experiment employs "zero applied field" resonance observed by microwave transmission at 9.232 GHz and requires a theory to relate the resonance signal to the magnetization, we discuss the question of fit to theory, determination of necessary parameters, etc., and conclude that the errors quoted here are statistical and not theory dependent. We determine a value for the critical amplitude B of 1.27 ± 0.03 and 1.23 ± 0.02 for the two samples, respectively.

I. INTRODUCTION

In this paper we describe an experimental measurement of the critical exponent β in polycrystalline and single-crystal nickel by an essentially new technique. β is defined by the limiting onset of magnetization $M(T)$ near the critical or Curie temperature T_C as

$$\beta = \lim_{\epsilon \to 0} \left(\frac{\ln M(\epsilon)}{\ln(-\epsilon)} \right),$$

where

$$\epsilon = (T - T_C)/T_C$$

denotes the reduced temperature. We say "essentially new" because, although we have previously described the method and have demonstrated its utility in an experiment on gadolinium,[1,2] this is the first measurement in which we can critically test the theory dependence of the measurement, assign a realistic value to its accuracy, and assess its overall significance.

Measurements of β in conducting ferromagnetic elements and alloys seem to be more difficult to do with the accuracy needed to compare to recent theory than, for example, similar measurements in insulating materials using optical methods, or with liquid critical-point behavior.[3-5] Measurements of β in nickel have been made by extrapolating to zero applied field the magnetization in a static magnetic field, and also by nuclear-moment "microprobe" methods such as nuclear-magnetic resonance (NMR) just below T_C, Mössbauer-effect measurements, or time-dependent perturbed angular correlation measurements. The former give values lower than ours and the latter give values somewhat higher. Although these other measurements cite accuracy comparable to ours, none of the measurements are consistent and some are not even self-consistent. We discuss these questions quantitatively in a later section.

By way of introduction, we discuss our technique in a qualitative fashion. It employs the microwave-resonance-transmission method. If we place a suitable conducting-metal sample as a common wall between two microwave cavities, one for the application of a microwave oscillating field H_1 on one side of the sample, and the other to match a transmitted signal on the other side to a coherent low-noise receiver system, the system is extremely sensitive only to the desired mode of magnetic resonance transmission and eliminates much of the noise originating in the source of the exciting H_1 field. This technique was first used to improve the observation of conducting electron resonance in new metals[6,7] and the literature on this subject of transmission electron resonance is, by now, quite extensive.[8]

Even if the magnetically resonant spins are not free to move and transport a resonance signal from one side of the sample to the other, as are the conduction electrons, there is another mode of transmission. We require a sample not so thick as to completely prevent some normal skin-depth leakage to be detectable as a signal in the second cavity. If the sample is ferromagnetic or paramagnetic and has a suitable magnetic field applied to it, the skin depth is modified because it depends not only on the electrical conductivity of the sample but also on its magnetic susceptibility. Even though there is only a small change in skin depth, the "e folding" of the effect through many skin depths produces a large measurable "resonance" on the receiver side of the sample. In practice nearly a watt may be applied at one side and the normal skin-depth leakage, which typically is only of the order of 10^{-15} W, may increase one

or two orders of magnitude at certain values of applied field.

One might use the words "magnetic dispersion skin-depth enhancement" to describe the effect. It is identical to "antiresonance" known in earlier ferromagnetic-resonance (FMR) experiments, but the effect is much more easily seen in transmission than in reflection. Physically, the enhanced transmission comes about because the spin system of the sample can store energy from internal fields and reduces the usual attenuation effects of the metal by Joule heating in the microwave eddy currents. We use the Maxwell eddy-current equation and some form of constituent resonance equations such as the Bloch-Bloembergen equation, the Landau-Lifschitz equation, or the Gilbert equation[2,9] to theoretically describe the effect.

Essential to our experimental measurement is that, whereas normal direct coupled magnetic resonance is determined by a resonance condition $\omega = \gamma H_0$ where γ is the gyromagnetic ratio and H_0 is the field inside the sample, the skin-depth enhanced transmission mode has a peak effect at a condition $\omega = \gamma B$, where B is the magnetic induction field inside the metal. Since $B = H + 4\pi M$, it is not necessary to have an externally swept magnetic field in order to obtain a resonance. Instead, one slowly drifts the temperature of the sample through the transition temperature, and by extracting the magnetization as a function of temperature, one obtains the necessary data for a value of β.

Aside from being a new experiment to compare to others, the advantage of such a method seems to be that it measures a true average value of magnetization sampled by the conduction electrons and that it is a true zero-field experiment. The disadvantage is that it is not (initially) clear that the theory dependence between the observed signal and the actual magnetization is sufficiently well established to interpret the signal and that the necessary parameters are available to provide a good measurement. An important part of this paper is a discussion of this latter point. We proceed, therefore, to details.

II. THEORY

A. Zero-field signal

The spin dynamics of a magnetic material are given by an equation of motion for the magnetization of the general form

$$\frac{d\vec{M}}{dt} = \gamma \vec{M} \times \vec{H}_{\text{eff}} + \cdots ,$$

where the dots represent relaxation terms. The first term on the right-hand side is just the torque exerted on $\vec{M}$ by $\vec{H}_{\text{eff}}$. H_{eff} may consist of several parts. It usually includes the actual H field seen by the magnetization M plus the effect of the exchange interaction written as an effective field $(2A/M_s^2)\nabla^2\vec{M}$. A is the exchange stiffness parameter, M_s is the value of the spontaneous (dc) magnetization. A detailed discussion of the contribution from this term to energy transport through the sample is given by Manikopoulos *et al.*,[2] and may be totally neglected in the transmission signal of nickel.

H_{eff} may also include the effect of an anisotropy energy. This occurs when there is a preferred direction for the alignment of the magnetization with respect to the crystal axes and is equivalent to an effective field in the "easy" direction. For nickel at moderate temperatures these are the [110] directions.[10] However, anisotropy fields rapidly approach zero for a cubic crystal near T_C and amount to no more than a few Gauss in nickel for $T \gtrsim 0.95\ T_C$.[10,11] Such effects may therefore be ignored in the critical regime.

Several forms of the relaxation terms have been applied in describing resonance phenomena in magnetic systems. A Bloch equation form

$$\left(\frac{d\vec{M}}{dt}\right)_{\text{trans}} = \gamma(\vec{M} \times \vec{H})_{\text{trans}} - \frac{\vec{M}_{\text{trans}}}{\tau} \tag{1}$$

was applied successfully to the transmission results of gadolinium by Alexandrakis *et al.*,[9] and is attractive because of its inherent mathematical and intuitive simplicity. $\vec{M}_{\text{trans}}$ stands for the components of M perpendicular to the static magnetization $\vec{M}_s$. τ is the phenomenological relaxation time arising from processes which cause $\vec{M}$ to return to its direction along $\vec{M}_s$ in the absence of an exciting field.

In FMR work during the last ten years it has been suggested that an alternate form, the Gilbert equation, seems best to describe the results of work done on transition metals and their alloys.[12,13] This equation is

$$\frac{d\vec{M}}{dt} = \gamma \vec{M} \times \vec{H}_{\text{eff}} - \frac{\gamma}{\gamma M_s^2}\left(\vec{M} \times \frac{d\vec{M}}{dt}\right). \tag{2}$$

The relation of the line-shape parameter λ to the Bloch relaxation time τ is roughly

$$\lambda\omega/\gamma M_s = 1/\tau ,$$

and is therefore like a relaxation time that depends on frequency and internal magnetization.

To determine the transmission of microwave energy through a metallic sample one uses such equations in conjunction with Maxwell's equations to obtain the wave vector for a solution that represents propagation through the material. A de-

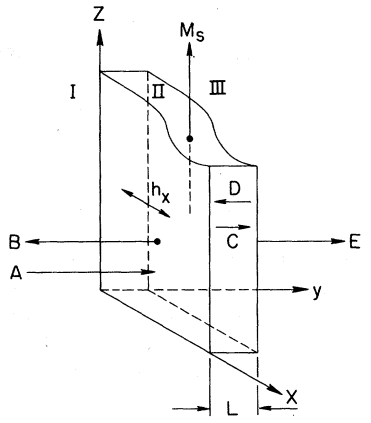

FIG. 1. Sample slabs showing orientation and notation used in the text. For regions I, II, III; L is the thickness; h_x is the incident rf field; M_s is the magnetization direction; and A-E are the propagation directions.

tailed calculation for the case of zero applied field was presented by Manikopoulos, Sheng, and Carver[2] by assuming Bloch-equation dynamics and the geometry indicated in Fig. 1. Their result gave a propagation vector with the form

$$k_2^2=(2i/\delta^2)[1+R^2/(i\Omega-\Lambda)^2], \tag{3}$$

where

$$\delta^2=c^2/2\pi\sigma\omega$$

and

$$R=\frac{M_s}{M_s(0)},\quad \Omega=\frac{\omega}{\gamma 4\pi M_s(0)},\quad \Lambda=\frac{1}{\gamma\tau 4\pi M_s(0)}.$$

$M_s(0)$ is the saturation magnetization at zero temperature. We can already see the existence of the enhanced transmission of electromagnetic energy from (3). For a nonmagnetic metal, we have $k_2^2=2i/\delta^2$, implying a $k_2=(1+i)/\delta$ that leads to the usual exponential damping of any electromagnetic wave as it travels into the material with a characteristic damping length or "skin depth" δ. In the magnetic case it is apparent that for small Λ, k_2 nearly vanishes when $\Omega\approx R$ implying no exponential damping of the signal and a resonance in transmission.

We can also obtain a solution for Gilbert-equation dynamics [Eq. (2)]. The wave vector in this case is given by the expression

$$k_2^2=\frac{2i}{\delta^2}\left(1-\frac{R^2-i\Omega\Lambda'}{\Omega^2(1+\Lambda'^2/R^2)-i\Omega\Lambda'}\right), \tag{4}$$

where R and Ω are as before, but

$$\Lambda'=\lambda/\gamma M_s(0).$$

Again, it is clear an enhanced transmission peak occurs near $\Omega\approx R$.

This phenomenon can be understood as follows: Normal propagation of energy through a metal involves a loss mechanism proportional to σE^2 as the $\vec{E}$ field causes currents to flow. In the magnetic material near resonance, where magnetic fields caused by currents couple to spins, energy is stored in the spin system and a new mode of propagation opens up that reduces the normal-loss mechanism.

To solve the actual problem of transmission we must match appropriate boundary conditions at the sample surfaces to determine the value of h_x on the far side of the slab. This is a general procedure. The results apply for any given system once the propagation vector k has been determined. Consider the situation shown in Fig. 1. The wavevector outside of the slab (regions I and III) is given by ω/c. In region II, we denote the wavevector by k. A, B, C, D, and E denote the amplitudes of the H field. By writing down the appropriate expressions for the continuous tangential components of $\vec{E}$ and $\vec{H}$ at the two surfaces in terms of these amplitudes one may solve for the transmitted amplitude E in terms of the incident amplitude A with the result

$$E/A=-i(c/\pi\sigma)k/(f_- - f_+), \tag{5}$$

where

$$f_\pm=(1\pm ikc/4\pi\sigma)^2\exp(\pm ikL).$$

Transmitted power is proportional to $|E/A|^2$. It is therefore possible to compute the expected signal from the value of the propagation vector k.

One can also obtain the reflected amplitude

$$\frac{B}{A}=\left[1+\left(\frac{4}{ck}\right)^2\right]\frac{\exp(+ikL)-\exp(-ikL)}{f_- - f_+}. \tag{6}$$

The absorption signal is proportional to

$$\frac{|A|^2-|B|^2}{|A|^2+|B|^2}=\frac{1-|B/A|^2}{1+|B/A|^2}.$$

In Fig. 2, the expected transmission for the Bloch and Gilbert equations of motion is plotted for values of parameters considered likely for nickel. The foil thickness was taken to be 26.2 μm (the actual thickness of one of the nickel foils to be used) and the conductivity, $\sigma=3.37\times10^{16}$ sec^{-1}, was obtained from a published value[14] for nickel at 325 °C($T\approx0.95T_c$). The saturation magnetization $M_s(0)$ is 510 G. The Gilbert relaxation parameter $\lambda=2.3\times10^8$ sec was obtained from FMR measurements fitted to this theory,[15] and a value of $\tau=3.4\times10^{-10}$ sec^{-1} in the Bloch equation was chosen to give the same value of transmitted power at the peak.

The curves are rather similar. Both predict the existence of a strong zero-field resonance

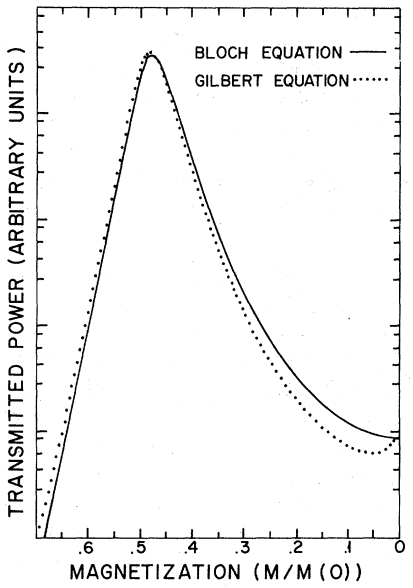

FIG. 2. Theoretical variation of transmitted power with internal magnetization. Horizontal axis is drawn in the direction of *decreasing* magnetization to denote direction of *increasing* temperature. Parameters used for the curves described in text.

with a peak at about the same value of the internal magnetization (near $R=0.48$) and with nearly the same width. Both curves converge to the value of transmitted signal for an ordinary (nonmagnetic) metal of conductivity σ at $R=0(T=T_C)$. Because these theories predict differences for small values of $R(T$ near $T_C)$, it should be possible to use our measurements to distinguish one from the other.

The procedure for extracting $M_s(T)$ from a measurement of transmitted power is now clear: We use a fitted theoretical curve $P(M_s)$ to assign a value of M_s to each temperature at which a given measurement of transmitted power is made.

We take care, however, to point out possible difficulties with this method. First of all, the determination of M_s is theory dependent and requires assumptions about the behavior of its parameters. For example, the conductivity σ varies significantly over the temperature range of interest so some form of $\sigma(T)$ must be incorporated into the analysis. We have further assumed that τ (or λ) is nearly temperature independent. That this might not be true is part of the motivation for considering transmission in applied fields discussed in a later section.

Also, as one approaches T_C, the resonant transmission becomes somewhat weak; nonresonant components of the transmission will begin to give a significant contribution to the signal. Furthermore, in setting up our equations we assume a certain orientation of M_s in the sample to the polarization of the rf field. Actually, the orientation of M_s will vary with different domains. The effect of domain structure in real samples is the subject of Sec. II B.

B. Domain structure

Domain structure is usually not important in magnetic resonance experiments at moderately high frequencies because the relatively high fields applied to observe the resonance signal are large enough to orient all domains in their direction. In materials with particularly strong anisotropy axes, this may not always be so; however, with iron and nickel an applied field of a few hundred Gauss is usually sufficient.

At zero field, however, we must take into account how the domains are likely to arrange themselves in the thin foils under investigation; a fascinating problem in itself and a subject of considerable study.[16] Although many of the details are of little consequence to our measurements, there are, however, a few important points. First of all, the magnetization will lie in the plane of the sample. This is an essential feature in the analysis of Sec. II A and follows from the fact that the magnetostatic energy density $-\frac{1}{2}\vec{M}\cdot\vec{H}$ is small for $\vec{M}$ in the plane and large and positive otherwise.

The second point is that one expects domains to extend through foils that are sufficiently thin. Following Kittel[17] and more recently Purtton[16] it appears that for nickel at high temperatures ($T \approx 0.9\ T_C$) domains will extend through foils less than about 100 μm thick. This greatly simplifies the analysis.

Nonetheless, one must still expect that $\vec{M}$ will be oriented in various directions within the plane and with respect to the exciting field for samples greater than about 1 μm thick. Further details of how $\vec{M}$ will arrange itself in the plane will be largely determined by the effective anisotropy fields present in the crystal.

To see what effect this has on the transmission signal we consider the case where the plane of the rf field h_1 is oriented at an angle θ with respect to $\vec{M}=M_s\hat{k}$. We write

$$\vec{h}_1 = h_1 \sin\theta\hat{i} + h_1\cos\theta\hat{k} \equiv h_{11}\hat{i} + h_{12}\hat{k}\,.$$

The transmission of the x component is described by our wavevector k_2. The transmission of the component of h_1 parallel to $\vec{M}$ can be shown to be nonresonant as in a nonmagnetic material; that is, $k_3^2 = 2i/\delta^2$. Thus h_{11} will propagate as k_2 and give an amplitude h'_{11} at the opposite side of the foil, whereas h_{12} will propagate as k_3 and give h'_{12}. Because of the nature of our apparatus, however

[parallel resonant cavities (see Sec. III B)], we will be sensitive only to the component of the transmitted signal parallel to the initial $\vec{h}_1$; that is,

$$h_3 = h'_{11}\sin\theta + h'_{12}\cos\theta .$$

The values of h'_{11}/h_{11} and h'_{12}/h_{12} may be obtained using Eq. (5) of Sec. II A with k_2 and k_3 substituted for k. We write

$$h'_{11}/h_{11} = \xi \quad \text{and} \quad h'_{12}/h_{12} = \eta .$$

Then $h_3 = \xi h_1 \sin^2\theta + \eta h_1 \cos^2\theta$ or

$$h_3/h_1 = \xi \sin^2\theta + \eta \cos^2\theta .$$

The experimentally measured value is $|h_3/h_1|^2$ or

$$P(\theta) = |\xi \sin^2\theta + \eta\cos^2\theta|^2$$
$$= |\xi|^2 \sin^4\theta + |\eta|^2 \cos^4\theta + (\xi\eta^* + \xi^*\eta)\sin^2\theta\cos^2\theta . \quad (7)$$

Near the resonance peak, $\xi \gg \eta$ and therefore the resonance curve will have precisely the shape given in the previous section. This justifies the statement that the transmission signal is largely insensitive to the details of the domain structure. However, both very near T_C, where $\xi \approx \eta$, and at low temperatures, where $\xi \leq \eta$, the curve will deviate from that shown in Fig. 2.

We consider Eq. (7) in more detail to see the three most probable cases that exist as a result of domain structure.

(a) *Case I.* Moderate anisotropy with one easy axis direction along $\vec{h}_1$. Here θ may assume the values 0°, 90°, 180°, and 270°:

$$P = \frac{1}{4}\sum_{\theta} P(\theta) = \tfrac{1}{2}(|\xi|^2 + |\eta|^2) .$$

This gives a signal which is equivalent to averaging the intensities of the resonant and nonresonant signals.

(b) *Case II.* Moderate anisotropy with easy axis at 45° to $\vec{h}_1$. Here θ assumes the values 45°, 135°, 225°, and 315°:

$$P = \frac{1}{4}\sum_{\theta} P(\theta) = \tfrac{1}{4}|\xi + \eta|^2 .$$

This gives a signal which is equivalent to summing the resonant and nonresonant amplitudes.

(c) *Case III.* Random orientation of domains or patterns where domains may assume all possible orientations. This is probably the case for no anisotropy. Then θ may assume all values with equal probability. Averaging over θ gives

$$P = \frac{1}{2\pi}\int_0^{2\pi} P(\theta)\, d\theta = \tfrac{1}{4}(|\xi|^2 + |\eta|^2) + \tfrac{1}{8}|\xi + \eta|^2 ,$$

which represents neither a simple sum of intensities nor amplitudes.

In Fig. 3 we compare these three cases using the Bloch equation parameters of Fig. 2. Except for overall scale factors, the three curves overlap very closely as expected in the vicinity of the peak. Away from the region of the peak, certain qualitative features suggest it may be possible to determine which case best describes the experimental results.

It appears desirable, therefore, to use single-crystal samples oriented perpendicular to a [100] direction so that the foils would contain both the easy [110] axes as well as the [100] axes. Either of these could then be oriented along the rf polarization.

For polycrystalline materials, often more readily available, one could hope to obtain reasonable results due to the small anisotropy mentioned. In such materials the orientation of the magnetization may be dominated by the crystallite size rather than domains. In this case, the orientation of the magnetization in each crystallite will try to line up with the easy axis in that crystallite that minimizes the magnetostatic energy of the entire sample. Although the magnetostatic energy will still favor the orientation of $\vec{M}$ in the plane, one might not expect that, for a crystallite size smaller than the sample thickness, $\vec{M}$ will have the same orientation from one side of the sample to the other. This can have a serious effect on the line shape. Further discussion of this matter will be

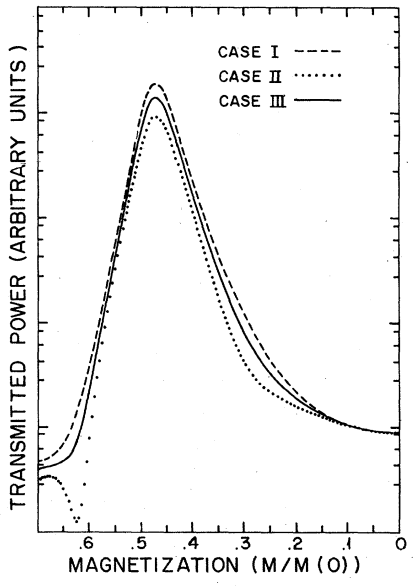

FIG. 3. Theoretical variation of transmitted power with internal magnetization for different domain structures. The definitions of the three cases shown, as well as the parameters used, are given in the text.

made when measurements on such samples are described.

C. Measurements in nonzero fields

One usually studies resonance phenomena by varying an applied magnetic field at fixed temperature and using the data to determine such resonance parameters as σ, τ, and the relevant g factor. All of these parameters are involved in our description of the zero-field resonance line shape; an accurate determination of each of them is crucial to the correct determination of $M_s(T)$ from the transmission data.

We would also like to determine, in as many situations as possible, whether the expected resonance behavior can be described by a consistent form of the spin dynamical equations of motion. By carrying out measurements in applied field at a variety of temperatures in the vicinity of T_C we gain valuable insight into both these questions. In particular, we find it easy to perform transmission measurements in an applied field perpendicular to the plane of the sample and such measurements allow a valuable comparison to be made between transmission and FMR in nickel at these temperatures.

The theory of the transmission signal for nonzero field was worked out by Alexandrakis[18] for the Bloch equation case. For a perpendicularly applied field H_A he found two solutions for the propagation vector, describing two circularly polarized waves along the applied field direction

$$k_p^2=\frac{2i}{\delta^2}\left(1-\frac{R}{\Omega-H+R+i\Lambda}\right), \tag{8}$$

$$k_n^2=\frac{2i}{\delta^2}\left(1+\frac{R}{\Omega+H-R+i\Lambda}\right), \tag{9}$$

where $H=H_A/4\pi M_s(0)$ and the remaining parameters are as previously defined. k_p and k_n refer to the (+) and (−) polarizations, respectively.

The first of these solutions leads to a resonance condition. For small Γ, the equality of Ω and H means that k_p becomes small and implies propagation of an unattenuated wave through the material. That is, when $H_A\approx\omega/\gamma$ one obtains the peak transmission.

The second solution, however, never becomes small and is nonresonant. Although the incident linearly polarized rf field will contain equal amounts of (+) and (−) polarization, the (−) polarization can be ignored in the vicinity of a strong resonance peak.

For some range of applied fields, however, this is not so and the contribution of both polarizations must be included for a meaningful analysis of the signal. By examining Eqs. (8) and (9) we see that for $H>\Omega+R$, the k_n transmission will actually dominate the k_p transmission. Near $\Omega=H$ our resonant solution becomes

$$k_p^2=(2i/\delta^2)i\Lambda/(R+i\Lambda),$$

which indicates the peak transmission decreases markedly with R. Thus, as one exceeds T_C and $R\to 0$, not only will the resonance become weaker but the region where k_n dominates the transmission will move closer to the resonance peak. Strictly then, contributions from both terms will be significant and we will include both as a matter of course for all of our analysis.

Two additional points should be made at this time. Firstly, one should be careful in using these equations close to the region where $H_A=0$. As previously stated, we need not worry about the effects of domain alignment for measurements made in applied fields. However, at lower temperatures where M_s is large, a field of some strength may be required to overcome the large magnetostatic energy tending to keep M in the plane. The value of H_A necessary to align $\vec{M}$ may be estimated from the energy density inside the foil $-\vec{M}\cdot\vec{H}_{in}$. Indeed, M will be aligned with H_A for $H_A\geq 4\pi M_s$. To satisfy this condition at the resonance peak, $H_A=\omega/\gamma$, for a frequency of 9.2 GHz, requires

$$M_s\lesssim\tfrac{1}{4}(3.06\text{ kg})=244\text{ G}$$

or $R\lesssim 0.48$ for nickel. Surprisingly then, even at moderately low values of M we must be careful to consider whether the observed line can actually be described in terms of k_n and k_p.

The final point concerns using the Gilbert equation instead of the Bloch equation in our analysis. For the kind of measurements being described, namely the observation of the transmission signal versus applied field at fixed temperature, the only essential difference will come from replacing of the Bloch linewidth parameter $1/\tau$ by $\lambda\omega/\gamma M_s$. Since ω and M_s are fixed for a given measurement it will be easy to distinguish among possible theories: By determining the linewidth parameter at a variety of temperatures we can ascertain whether it is essentially constant (the Bloch-equation statement), varies with temperature as $1/M_s(T)$ (Gilbert-equation case), or exhibits anomalies near T_C such as those suggested recently by other workers.[19]

III. EXPERIMENTAL APPARATUS

A. Microwave system

Since a thorough description of the microwave system has been given elsewhere[7,18,20] we give only a brief description here.

We use a V58C Varian Klystron to produce about

700 mW of microwave power at 9.2 GHz. Because the receiver used to detect the transmission signal is very sensitive, the Klystron is phase locked to a 540A Hewlett-Packard transfer oscillator to provide frequency stability and reduce noise. The receiving system is a superheterodyne detector which employs a local oscillator signal created by generating a sideband on a few milliwatts of the Klystron output with a 30-MHz i.f. in a double balance mixer. The entire system is therefore phase coherent and the output of the detector is sensitive to phase shifts present in the transmission signal itself. In certain applications a continuously rotating phase shifter is employed immediately before the sideband generation; this gives a sinusoidal varying output whose envelope is proportional to the signal amplitude. In the case of the work on nickel, this feature was used almost exclusively.

We describe briefly the method employed to observe and measure the transmission signal. A thin metallic sample of 15 to 20 skin depths thick is sandwiched between two microwave resonant cavities tuned to the fundamental Klystron frequency ν_0. Incident microwave power of about 300 mW is sent into one cavity; the transmitted power is picked up in the second cavity and sent to the heterodyne detector.

Before each measurement or series of measurements we switch to a "calibrate" mode of operation where a calibrated attenuator sends a known fraction of the Klystron output to the receiver. Then the switch is set to observe the transmission cavity and the actual signal is compared directly with the calibration. This method is valuable to discriminate against any long term drifts of the Klystron output power or detector. The variable attenuator may also be used to check overall linearity of the detector and therefore allow measurements to be made over a wide range of signal intensity using only a few calibration settings for comparison. This technique is especially useful while drifting temperatures to plot transmitted power against temperature.

B. High temperature cavity system

The microwave cavity system shown in Figs. 4 and 5 consists of two identical microwave cavities, $1\frac{1}{8}$ in. long, $\frac{1}{2}$ in. wide, and $\frac{3}{4}$ in. deep, resonant in the TE_{101} mode at about 9.22 GHz. Each cavity is provided with a variable dielectric tuning rod and coupler as shown. The sample is sandwiched between them and between two metal sample plates (described below) to form a common wall between both cavities in a region where rf fields are the most intense. The cavity block is made from solid copper for high electrical conductivity and thermal stability. The loaded cavities have a modest Q of about 2500 at room temperature and 2000 at the temperature of interest.

The Curie temperature of nickel (about 360 °C) is sufficiently high to require care to protect the cavity and sample surfaces from oxidation. During measurements the entire assembly was enclosed within a copper can sealed to contain an inert atmosphere of helium or argon. The gas was purified by a Centorr Model 2B titanium gettering furnace designed to reduce any reactive impurities to less than 0.01 ppm.

The cavity construction reflects the requirement of being able to operate at relatively high temperature: Hard soldering and ceramic cement[21] were the rule; pieces that needed to be disassembled were joined with aluminum wire seals; dielectric materials were made of fused quartz; electrical connections were made through ceramic metal feedthroughs.[22]

The temperature scan near the critical region caused enough change in cavity dimensions to require they be retuned after every interval of several degrees. Moreover, after an interval of about 30° the coupling had to be readjusted to compensate for coupling hole changes and changes in the cavity Q. Though potentially more serious in destroying

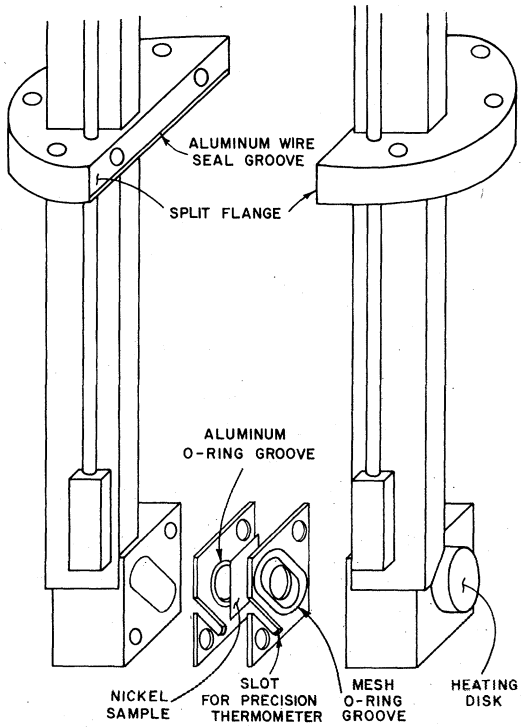

FIG. 4. Perspective and separated view of two-cavity system showing locations for thermometry and split-flange structure. Outer can and heater not shown.

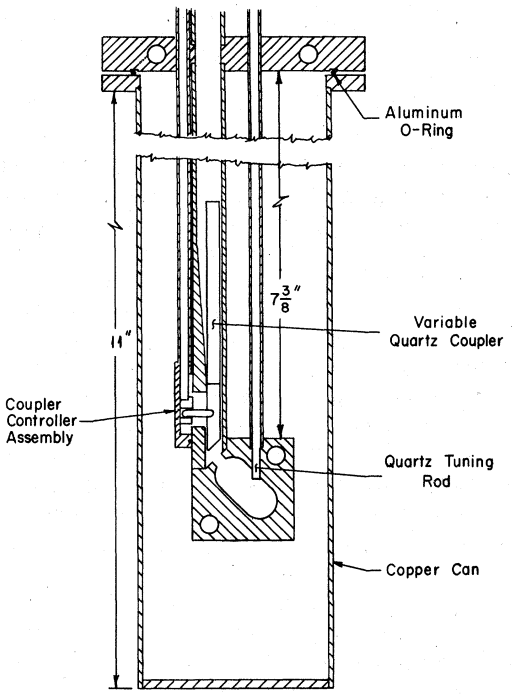

FIG. 5. Cross section of cavity structure showing details of cavity tuning and coupling devices. Sample retaining plates not shown.

signal calibration the latter effect was not large (a few percent) over the most important temperature range.

A significant problem was the deformation of the sample plate assembly which had to provide good electrical contact between the samples and cavities. Since the second cavity had to be isolated from the first to better than 150 dB, even the smallest break in these seals would give enough leakage to mask the real signal. The problem was solved by providing each sample plate with a 0.020-in.-diam aluminum wire O-ring on the sample side and a $\frac{1}{8} \times \frac{1}{16}$ in. wire mesh gasket[23] normally used to join waveguide flanges on the cavity side. The wire mesh deforms reversibly and takes up any distortion in the rest of the assembly without distrubing the aluminum seals.

The system was used many times and performed flawlessly up to temperatures of 400 °C. The main heating was provided by a 400-W Electrothermal heating tape attached to the copper can. Since this tape was powered by a stable dc supply and was noninductively wound, only a 0.5 G field was ever detectable in the cavity region.

Helium was chosen for the inert inner atmosphere because of its high thermal conductivity. A calculation of the heat flow into the cavity block from the flange through the waveguide and by the helium exchange gas showed roughly equivalent results. The large thermal mass of the copper cavity block insured that a 5° difference between the outer can and the cavities themselves leads to less than a 10-mdeg temperature gradient across the sample. In practice, no temperature difference across the cavity block could be detected.

C. Temperature measurement and control

The primary thermometer used in the critical regime of nickel was a four leadwire platinum resistance device, supplied by Minco Products, Inc.,[24] which was positioned within the sample plate assembly to be as close to the sample as physically possible. The strain-free platinum element was calibrated in the temperature range 300–400 °C and said to have an absolute accuracy of ±0.6 °C at 300 °C and ±0.7 °C at 400 °C. The repeatability over this range was stated to be ±0.05 °C. During each run, relative temperature readings are valid to at least this precision, probably to ±10 mK.

An ac bridge circuit was used with this thermometer to avoid the effects of dc offset voltages, to minimize self heating, and maximize sensitivity. A change in resistance in the thermometer corresponding to a temperature change of less than 5 mK was readily observable. In several runs with the same sample the positions of the various features of the observed signal remained constant to within 0.1 °C.

For measurements in zero applied field, the cavity system was allowed to drift slowly in temperature and no temperature-control functions were necessary. For measurements in an applied field at fixed temperature, however, a control was needed to keep the temperature constant over an extended period of time. For this we used two additional heating units attached directly to the cavity block which could supply 12 W of power (see Fig. 5).

The heating disks were placed symmetrically on the cavity block to ensure that no temperature gradients would develop in the sample plane. A small platinum-resistance thermometer[24] was imbedded in one of them approximately 1 mm from the heating element itself. This insured that thermal lag is minimized between the heating and sensing parts of the system to stop oscillations.

The actual temperature-control unit was partly modeled after a unit designed and built by Griffin.[25] It has been used at cavity temperatures up to 370 °C. During the time required for a magnetic field scan the regulation was 50 mK or better.

D. Sample preparation

The polycrystalline and single-crystal nickel samples used for the actual measurements came

from two different sources. A 0.010-in.-thick 99.999%-pure polycrystalline foil was obtained from Research Organic/Inorganic Chemical Corp. A 0.035-in.-thick, 0.5-in.-diam (100) single-crystal piece of nickel was generously provided by W. Flood of Bell Labs.

The single-crystal piece was cut into two 0.015-in. sections with a Lastec Model 2006A wire saw. The sections were ground to about 0.007 in. using fine emery paper.

A chemical lapping technique suggested to us by Paul H. Schmidt of Bell Labs was used for the final reduction in thickness. The samples were mounted with glycol thalate wax on a special high-precision machined stainless-steel lapping holder[26] which exposed the samples at steps of 25 μm to an acid-impregnated surface. The acid etchant used was a mixture of three parts nitric, one part sulphuric, one part phosphoric, and five parts acetic acid, also suggested by Paul H. Schmidt. This etchant was poured onto a double layer of fiberglass cloth stretched on a flat glass table. The glass was heated to 90 °C to increase the chemical activity of the etchant.

The lapping of each fact was done by hand, using a figure-eight motion on the wet cloth and rinsing in cold water at approximately 20-sec intervals. Thickness was determined by a precision micrometer, accurate to 2.5 μm. The variation of thickness of the finished samples was no greater than this. X-ray pictures of the single-crystal pieces confirmed the (100) orientation and identified the crystal axes for alignment to the cavity geometry.

IV. EXPERIMENTAL RESULTS

A. Zero-field results

The technique for obtaining the zero-field transmission signal as a function of temperature has already been described in Secs. I–III. The cavity system is allowed to drift slowly in temperature in one direction over the region of interest. Before each measurement of transmitted power a calibration signal is recorded and both cavities are retuned and recoupled if necessary. Then the transmitted signal is recorded and the temperature recorded. Since approximately 15 sec are required to get a good signal reading, the accuracy of the temperature is determined primarily by the amount of drift during this period. Typically this gives ±0.1 °C.

The accuracy of the transmission signal depends on a couple of factors. At best it is limited by the accuracy of the recording instruments used to observe the calibration and transmission signals. This gives roughly a 2% error. When observing signals over many orders of magnitude in intensity, however, additional systematic errors arise from the attenuator providing the calibration signal. A setting on the attenuator giving 100-dB attenuation of the incident power level was chosen to represent a signal of unit intensity. Although readings within 20 dB of this level were determined accurate to a few percent, uncertainties in the absolute calibration level were found to increase steadily as higher attenuation settings were used.

To avoid ambiguities in domain structure all temperature scans were made by first increasing the temperature to above T_C and the allowing the cavities to cool slowly. Incongruities noted in some preliminary measurements could be entirely attributed to changes in domain structure caused by rapid changes of the anisotropy constants and magnetization from their low-temperature values.

For the measurements on the polycrystalline sample we also found it necessary to apply a small bias field to control the way the individual crystallites would "freeze in" the direction of their magnetization in cooling below T_C. In Sec. II, we noted that a meaningful analysis depended on having a uniform direction of magnetization extending across the foil. In the case of the sample studied, applying a 10-G field in the sample plane seemed sufficient to get good results. For the single-crystal sample no such bias field was used.

In Fig. 6 the experimental results are shown for a 26.2-μm polycrystalline nickel sample at a microwave frequency of 9.202 GHz. The signal intensity is plotted on a logarithmic scale. The crosses shown for the individual data points correspond to an uncertainty of two standard devia-

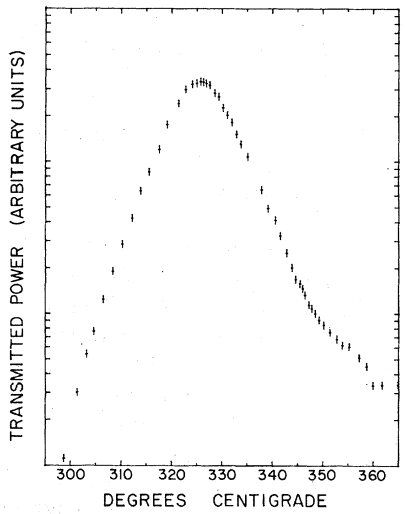

FIG. 6. Transmitted power vs temperature for a 26.2-μm-thick polycrystalline nickel foil. Critical temperature is at discontinuity at right.

tions in temperature and signal power; that is, roughly to ±0.2 °C and a 5% signal uncertainty, respectively. The curve flattens out for temperatures above T_C where the magnetization is no longer changing. From several runs using the same sample we obtain $T_C = 359.7\,°C \pm 0.1\,°C$. This value of the Curie temperature agrees with that observed for the highest-purity nickel samples measured by other workers.[27]

These data represent the first observation of a zero-field resonance in nickel. We see that the peak of the curve is very sharp and occurs at roughly 325.5 °C or at a reduced temperature of 0.054. Thus the entire region of the resonance peak lies within a temperature regime very close to T_C.

We next determine the relevant resonance parameters to compare these data with the theory, thereby also extracting a value of the critical exponent β. Recalling the discussion of Sec. IIA we observe, first of all, that the monotonic rise in the experimental curve immediately below T_C clearly favors a Bloch-type theory over the Gilbert description. The decrease in intensity just below T_C for the Gilbert solution shown in Fig. 2 cannot be reconciled even with domain considerations—it is a basic feature of that theory. This feature is simply not present in the experimental data.

Therefore, the analysis is attempted using the Bloch-equation results. Because this was a polycrystalline sample we omit any consideration of domain structure. As we discussed in Sec. IIB, such considerations should not be important over the range where there is a strong resonant signal.

Basically there is only one parameter to be determined: the value of the relaxation parameter τ. The value of the conductivity is taken from dc measurements on high-purity nickel in this temperature range.[14] Because some workers have reported that the conductivity at microwave frequencies may be lower than the dc value[7,9] some effort was made to justify this assumption comparing the transmission just above T_C to the transmission by a slightly thicker foil from the same sample (40 μ) and to aluminum foils of 6.5 and 12.5 μm at room temperature. All of these results indicated a microwave conductivity for the nickel sample consistent with the dc value at T_C: $\sigma = 3.0 \times 10^{16}\ \text{sec}^{-1}$. We therefore obtained $\sigma(T)$ over the entire temperature range from the dc measurements. The value of the g factor was taken to be 2.2 from FMR measurements;[28] the saturation magnetization $M(0)$ of nickel is 510 G.[29]

Since the theoretical description relates the transmitted power to the internal magnetization $P(M)$ determining τ required some assumption to be made about the value of internal magnetization. At the same time, such an assumption could not be allowed to prejudice the final result for $M(T)$. This was accomplished in the following way: For a given value of τ the theory was used to predict the value of M corresponding to the resonance peak. Then a probable value of β was assumed to give $M(T)$ in the $\frac{3}{4}$ maximum region of the peak and thereby compute a value of χ^2 for the 11 data points in this region. This was repeated with different values of τ until a best fit was determined. Because the resonance was so narrow, these data points all lay within a ±4 °C range and a single value of conductivity (that of the peak) was used. Using such a small temperature range allowed the guessed value of β to be varied from 0.34 to 0.38 without affecting the best value of τ. These values of β encompass those previously measured in other experiments.

The value for τ thus determined was $2.86 \times 10^{-10} \pm 0.11 \times 10^{-10}$ sec. From the value of M at the resonance peak of $M(T)/M(0) = 0.471$, the corresponding value of the Gilbert parameter λ may also be determined. It is $\lambda = 2.74 \times 10^8\ \text{sec}^{-1}$, which may be compared to the value $2.3 \times 10^8\ \text{sec}^{-1}$ from FMR measurements.[15]

With this value of τ the theoretical relation $P(M)$ may now be used to determine $M(T)$ for the entire temperature range. The value of transmitted power at the peak is normalized to the theory for that value of σ and τ and $M(T)$ is determined for each temperature T_i from the known values of $\sigma(T_i)$, $P(T_i)$ and (const) τ. We then convert T_i to a reduced temperature using our value of T_C to give $M(\epsilon)$.

In Fig. 7 we plot $\log_{10} M$ vs $\log_{10} \epsilon$. The error bars shown reflect an uncertainty in ϵ caused by the 0.1 °C uncertainty in T and T_C while the uncertainty in M comes from the 2% uncertainty in P. The data do, in fact, lie in a straight line for ϵ between 2×10^{-2} and 1×10^{-1}. A least-squares fit for the data in this range determines β to be 0.357.

The uncertainty in this value of β comes from two major sources. First, the uncertainty in τ gives

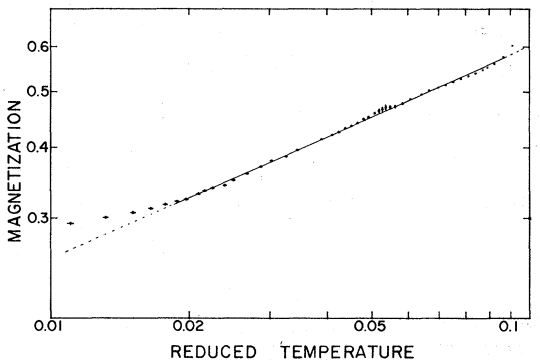

FIG. 7. Log-log plot internal magnetization vs reduced temperature for polycrystalline foil. The slope of fitted line (β) is 0.357.

a deviation of ±0.006. Second, an uncertainty in the thickness of the foil, of ±0.00005 in or ±5%, also can lead to an error of ±0.006 in β. The combined uncertainty gives $\beta = 0.357 \pm 0.008$ for $10^{-2} < \epsilon < 10^{-1}$.

It is interesting that uncertainties in the g factor or the value of $M(0)$ have no effect on the value of β. By examining Eq. (3) it is apparent that a changing in either γ or $M(0)$ can be compensated by rescaling R by a corresponding amount. This will not affect β as long as this rescaling factor is constant in temperature.

The remarkably small deviation of the data points from a straight line over a temperature range extending 20 °C on both sides of the transmission peak is a strong argument for the validity of the theory. The deviation of the points below $\epsilon \approx 2 \times 10^{-2}$ is just the result of the nonresonant contribution to the signal discussed in Sec. II B which becomes significant as the resonance becomes weak. Unfortunately, there is no way to take this contribution into account in the polycrystalline case without introducing extra *ad hoc* assumptions. Indeed, at temperatures somewhat below T_C a large variation of signal was produced by changing the bias field by only a few Gauss. This indicated a largely undefined magnetization geometry in spite of the presence of the bias field.

The true test of the theory seemed possible by using a single-crystal sample. It was of interest to obtain meaningful measurements over a temperature range sufficiently below the resonance region to observe the effect of the nonresonant propagation. As a final check on these measurements, one single-crystal foil was actually hard soldered in place between the two sample plates to be sure that the relatively weak signal contained no contribution from spurious leakage.

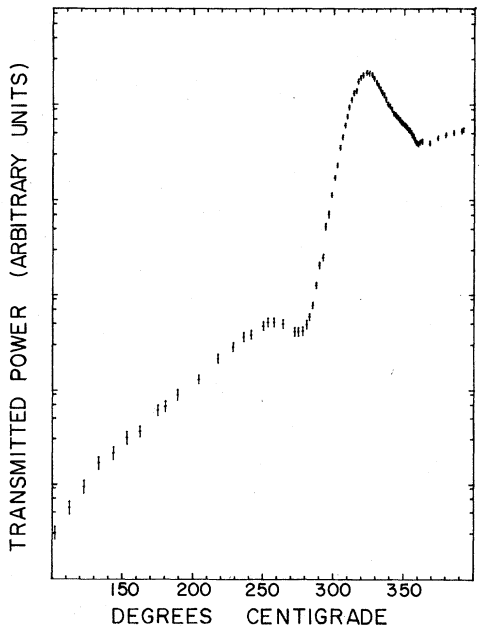

FIG. 8. Transmitted power vs temperature for a 35-μm (100) oriented single-crystal nickel foil. The change of nonresonant baseline slope and interference effects at sides of line are discussed in text.

The results of a run taken on a 35-μm (100) single-crystal foil are shown in Fig. 8. The frequency used was 9.232 GHz and one [100] crystal axis was oriented parallel to the polarization of the rf H field. These data, extending between 100 and 400 °C, were again taken by drifting downward in temperature. The transmitted power is plotted on a logarithmic scale and extends over five orders of magnitude. The increase in the size of the power-level error bars at low levels reflects the larger systematic uncertainty when using higher attenuation settings of the calibrated attenuator. The value of T_C appears to be 359.0 ± 0.2 °C from these data.

The contribution from the nonresonant component of propagation is evident. The slope of the base line merely indicates the temperature variation of conductivity; that is, for the nonresonant propagation,

$$P \propto \exp(-2L/\delta),$$

so that

$$\ln P \approx K - (2Lc/2\pi\omega)\sigma^{-1/2}(T),$$

where L is the foil thickness and K is essentially constant in temperature.

The points above the Curie temperature are also due to nonresonant transmission and obey such a relation. The slope of a straight line joining these points is less than that of a line joining the low-temperature points. This reflects the well known change in slope of the resistivity curve at a magnetic change of state. The level above T_C is also somewhat higher than that obtained by extrapolating the low-temperature line to T_C. This occurs because above T_C the entire signal is transmitted nonresonantly; below the resonance region only the component of the rf field paralleled to M will contribute to the transmitted power.

No bias was applied in obtaining these data. Spurious fields from the heating tape and Earth's field amounted to no more than 1 G. On subsequent runs the effects of applying small bias fields up to 100 G in the plane of the sample were observed. These effects were quite small. This supports the conclusion reached in Sec. II B that domains would extend from one side of the sample to the other.

It thus seemed justified to analyze these results using the multidomain theory of Sec. II B. In that section three possible cases for domain structure

were considered. Ideally, by comparing the transmission level to T_C to the extrapolated low temperature line, one can distinguish among these three cases. Such a comparison favors case III, that of a random orientation of magnetization. This somehow seems intuitively the most likely near T_C where the anisotropy is negligibly small. On the other hand, the apparent interference effect between the resonant and nonresonant components on the low-temperature side of the peak suggests that at these lower temperatures there is a tendency for the magnetization to line up along the [110] axes. This is the "easy" axis of magnetization for nickel at these temperatures.

Since we are most interested in the behavior close to T_C, we assume a random orientation of magnetization in our analysis. Once again there seems no evidence suggesting the Gilbert equation kind of behavior near T_C. Therefore we again assume Bloch equation dynamics with a constant value of τ.

Several features of these data suggest a value of the conductivity differing substantially from the dc data. Fortunately, the nonresonant base line itself may be extrapolated to infer $\sigma(T)$. That is, from the slope of this line one can infer the change in skin depth with temperature to be

$$\frac{1}{\delta(T)} = \frac{1}{\delta(T_C)} + \frac{(2.95\times10^{-2})/°\mathrm{C}}{2L}(T_C - T),$$

where $(2.95\times10^{-2})/°\mathrm{C}$ is just the slope of $\ln P(T)$ for the nonresonant base line. Given a value of $\sigma(T_C)$, $\sigma(T)$ may be determined for lower temperatures from this relation.

The data are fitted to the theory as follows: One chooses a value of $\sigma(T_C)$ and computes the value of τ that gives the correct peak transmission. One then varies β to find the best fit for some collection of data points. We chose 30 points approximately equally spaced in temperature between 310 °C and T_C. One then searches for the best overall fit to such sets of σ, τ, and β.

The result is shown in Fig. 9. The values of the parameters obtained were $\sigma(T_C) = 8.4\times10^{15}$ sec^{-1}, $\tau = 1.82\times10^{-10}$ sec, and $\beta = 0.358$. The error bars shown on the data points represent about two standard deviations. The agreement between theory and experiment is very good. For the 2% average deviation in the experimental points, the three-parameter fit gives a reduced χ^2 of 0.88. Since we have used σ as a fitting parameter, uncertainties in the sample thickness are not important. Thus the uncertainty in β is determined solely from the fitting statistics; it is ±0.003.

A plot of $\log_{10}M$ vs $\log_{10}\epsilon$ can be constructed as in the polycrystalline analysis. This curve is shown in Fig. 10. The error bars reflect the ±0.2 °C uncertainty in T_C, the ±0.1 °C uncertainty in each

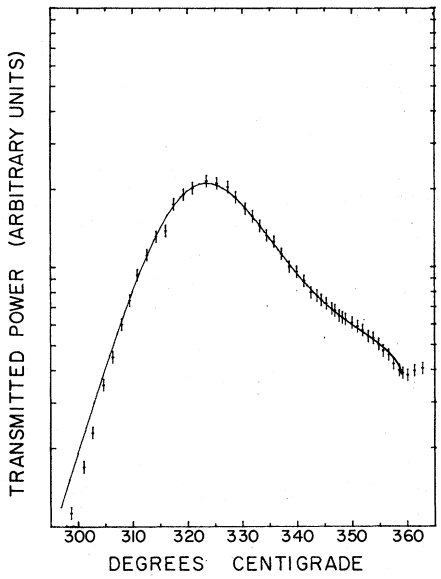

FIG. 9. Transmitted power vs temperature for single-crystal foil showing theoretical fit to deduce parameters: $\sigma(T_C) = 8.4\times10^{15}$ sec^{-1}, $\tau = 1.82\times10^{-10}$ sec, and $\beta = 0.358$.

temperature point, and the 2% uncertainty in power level. We see that the curve follows a straight line over a temperature range $5\times10^{-3} < \epsilon < 10^{-1}$.

One interesting result from the analysis is the low value obtained for the conductivity σ. Although surprising, it is entirely in agreement with several other features of these data. During the actual measurements it was noted that the transmission signal was much larger than expected. When compared to the polycrystalline runs and aluminum-foil test samples the absolute level of the signal indicated a skin depth of roughly 5.5 μm, or almost twice that based on the dc data. Second, the slope of the nonresonant lines shown in Fig. 8 agrees both above and below T_C with the dc data when these

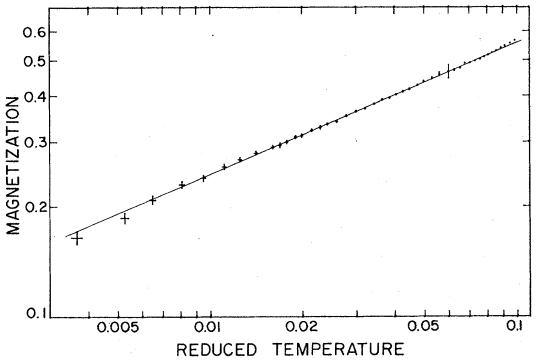

FIG. 10. Log-log plot of internal magnetization vs reduced temperature for single-crystal foil data. Slope of fitted line (β) is 0.358.

data are rescaled to make $\sigma(T_C) = 8.2 \times 10^{15}$ sec^{-1}. Finally, the difference in transmitted power at T_C of a 37.5-μm foil from the single-crystal sample compared to the 35-μm foil was also consistent with a skin depth of 5.5-μm. The skin depth expected from the dc data, consistent with the polycrystalline results, is 2.87-μm.

This low value of σ is reminiscent of the low values of σ obtained by other workers at microwave frequencies mentioned previously. It remains, as yet, unexplained. However, the lower value of τ also obtained suggests that it may be associated with impurities which have a more pronounced effect at these frequencies than at dc. Along these lines we note that the value of T_C for this sample was lower than that of the polycrystalline sample, but only by 0.7 °C. Typically this would suggest an impurity level of only 0.06%.[30]

The agreement in the value of β for the polycrystal and single-crystal samples is stunning. It is particularly noteworthy that the analysis of the zero-field transmission signal, assuming a constant value of τ, has yielded such a good fit to the data and a consistent value of β to temperatures very close to T_C. At least for measurements in zero field it would appear that the main contributions to the resonance relaxation mechanism are essentially temperature independent. This conclusion will be considered further in Sec. V.

B. Applied field results

A series of measurements were made using a 40-μm foil from the polycrystalline nickel sample in a perpendicularly applied magnetic field. At fixed temperature the applied field was swept from 1 kG to about 3.5 kG and the transmitted power was recorded. The magnetic field was monitored with a Bell Model 460A Incremental Gauss Meter and calibrated probe, accurate to 1%. The probe was positioned as close to the cavity system as possible while still avoiding the high temperatures of the cavity heating system. Afterwards an NMR probe[31] positioned in the region previously occupied by the cavities verified the readings of the Hall probe to within 1%.

The rationale for using a thicker foil than in the zero-field measurements was that one thereby obtained a more easily interpretable line shape over a larger temperature range. That is, we found it advantageous to suppress the contribution of the non-resonant transmission particularly at temperatures above T_C where the resonance signal was weak. This was accomplished by using a thicker foil.

Measurements were made on this foil for temperatures between 330 and 361 °C over several days. Between runs taken on successive days the signal characteristics changed slightly, indicating a slow deterioration of the resonance line-shape parameter. Since on a given day the sample was often kept at high temperatures for as long as 10 to 15 h (to allow thermal stabilization at each fixed temperature) this slow deterioration is probably not surprising.

For each field sweep, a few calibration signals were recorded that were comparable in intensity to that of the transmission peak. From the observed signal intensity and resonance width the values of the internal magnetization M and linewidth parameter τ could be calculated for each temperature. This value of magnetization corresponds to the resonance peak itself and therefore includes the sum of both the spontaneous and dc induced contributions in an applied field of approximately 3 kG. From the value of τ and M the value of the Gilbert parameter λ is also obtained.

The results for $M(T)$ are shown in Fig. 11. The error bars reflect the uncertainty in the relative power levels (the level at the transmission peak varied five orders of magnitude in this temperature range) and an uncertainty of ±10 to ±20 G in the resonance width. Note the deviation of the curve for temperatures below about 342 °C. The value of the magnetization at this temperature

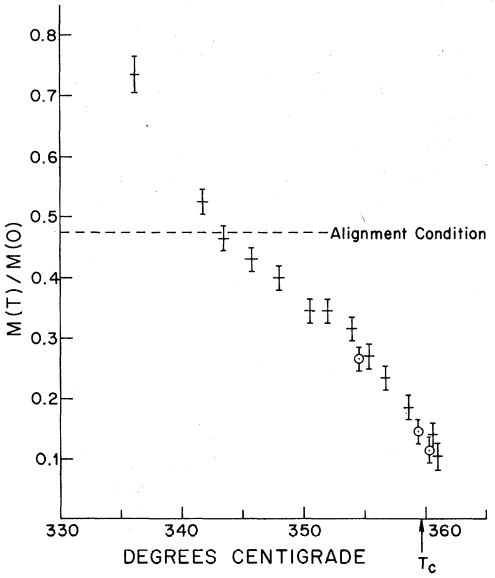

FIG. 11. Temperature variation of internal magnetization in an applied field of 3 kG for a 40-μm polycrystalline nickel foil. Circled and uncircled data points indicate data taken on different days. Results of this analysis are invalid for an internal magnetization greater than about 0.48 due to the inability of the applied field to align M perpendicular to the plane ("Alignment Condition").

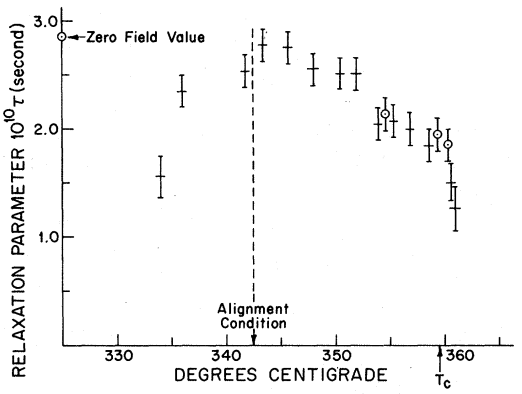

FIG. 12. Temperature variation of the relaxation parameter τ characterizing the transmission in a perpendicular applied field.

$[M(T)/M(0) \approx 0.47]$ is almost precisely where, as discussed at the end of Sec. IIC, we expect our theoretical analysis to break down due to the failure of the applied field to completely align the magnetization. Indeed, below this temperature the resonance line was noticeably distorted.

The temperature variation of τ and λ is shown in Figs. 12 and 13, respectively. The error bars correspond to the uncertainties in the resonance width mentioned above. Again there is a deviation in the curves below 342 °C. We have indicated the value of the line-shape parameter deduced in Sec. V A for the zero-field resonance. This value most appropriately corresponds to the temperature of the zero-field peak, about 325 °C.

The g factor was found to be 2.24 ± 0.02 over the temperature range 342–358 °C. This value is generally consistent with those obtained by FMR measurements of 2.22 ± 0.02.[28,32] In some FMR studies it appeared there might be an increase in the g factor at T_C. For example, a measurement by Salamon,[33] while giving the value of 2.22 below T_C, gave a value of 2.29 ± 0.02 above T_C. There are indications that a similar increase may also be present in the transmission data. New measurements are currently being made to investigate this matter further.

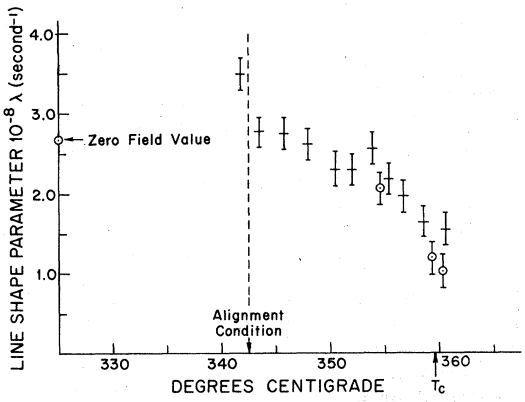

FIG. 13. Temperature variation of the line-shape parameter λ characterizing the transmission in a perpendicularly applied field.

The values of the line-shape parameters τ and λ shown in Figs. 12 and 13 both display considerable temperature variation. The value of τ does appear to remain relatively constant to about 350 °C and agrees fairly well with the value obtained at zero field. It does not, as expected by the Gilbert statement, decrease in temperature as rapidly as the internal magnetization. However, it is not quite as constant as the analysis of the zero-field results seem to suggest.

The Gilbert parameter λ appears to vary even more markedly with temperature. This seems to imply that the dominant contribution to the relaxation mechanism is, in fact, temperature independent. Some recent FMR measurements made in nickel also suggest a deviation in this manner from a constant value of λ for temperatures in excess of $T \gtrsim 0.9T_C$.[15]

These results, therefore seem to favor the Bloch-equation description of the transmission signal of nickel in this temperature regime. In particular, the analysis of the zero field polycrystalline data using a fixed value of τ seems justified at least to temperatures of perhaps 350 °C. Some restraint, however, must be taken in applying these applied field results too freely to the measurements taken in zero field. The thermodynamic behavior of the magnetization is quite different in zero field than in the presence of an applied field of 3 kG, especially for temperatures approaching T_C. One might guess that critical fluctuations in the absence of an applied field near T_C could give a considerable contribution to the relaxation rate so that an applied field, which destroys the critical behavior, would tend to increase the value of τ. Surprisingly, from our detailed analysis of the single-crystal zero-field line shape, the opposite seems to be true; that is, the assumption of constant τ seems to be even more valid. This matter will be considered a bit further in Sec. V.

V. CONCLUSIONS

In Sec. IV, a value for the critical exponent for nickel was dedetermined by analysis of the zero-field resonance line shape. This value is $\beta = 0.358 \pm 0.003$ for a reduced temperature $5 \times 10^{-3} < \epsilon < 1 \times 10^{-1}$. From our measured value of the g value the critical amplitude B may also be determined. It is 1.23 ± 0.02 for the single-crystal sample. (A slight-

ly higher value of 1.27 ± 0.03 is obtained from the polycrystalline results.)

It is worth mentioning that for the single-crystal data the analysis was entirely self-contained; i.e., it was possible to obtain all of the parameters relevant to this determination of β from the zero-field data alone. In addition, it is important to note that the value for T_C was obtained from qualitative features of the data independently of the fitting procedure used to determine the exponent. The more customary procedure of using T_C as a fitting parameter (that is, of choosing a value of T_C that seems to give the most consistent value for the exponent) can sometimes lead to erroneous results due to the large correlation of the exponent to the chosen T_C. We now wish to compare our value of β with those obtained most recently by other workers.

As mentioned in Sec. I, this exponent has been measured in nickel by a variety of methods. A direct measurement of the magnetization in bulk samples of nickel and nickel-copper alloys using an applied field extrapolated to zero[34] gave a value $\beta = 0.346 \pm 0.007$ for $2.4 \times 10^{-5} < \epsilon < 5.6 \times 10^{-3}$. Additionally, a number of measurements have been made using hyperfine probes. NMR measurements on the ^{61}Ni isotope occurring in natural nickel samples[35] yielded a value of 0.336 ± 0.002 for $4 \times 10^{-2} < \epsilon < 10^{-1}$. Unfortunately, it was found that the NMR line shape deteriorated prohibitively in the vicinity of T_C and could not be interpreted very close to the critical regime. Two other kinds of hyperfine measurements were made with impurity nuclei. Mössbauer measurements[36] on impurity ^{57}Fe gave $\beta = 0.378 \pm 0.010$ for $3 \times 10^{-4} < \epsilon < 4 \times 10^{-2}$ and perturbed-angular-correlation measurements of the two γ decay of ^{100}Rh imbedded in nickel samples[37] produced a value of $\beta = 0.385 \pm 0.005$ for $10^{-4} < \epsilon < 10^{-1}$.

The consistency of the last two measurements led these workers to conclude that they were, in fact, measuring bulk critical exponents via their hyperfine probes. The assumption that the critical behavior of the hyperfine field will follow $M_s(T)$ has periodically been called into question.[38] A recent measurement using time-dependent perturbed angular correlation on impurity ^{181}Ta in nickel[39] giving $\beta = 0.417 \pm 0.010$ for $5 \times 10^{-4} < \epsilon < 2 \times 10^{-1}$ suggests that equality between hyperfine and bulk β exponents does not always occur. The value of β obtained in the present work disagrees with all of the hyperfine measurements.

Often, upon the determination of a critical exponent by some new measurement, an attempt is made to reconcile this value to the predictions of scaling theory by comparing it with other measured exponents. Then, in some cases, these values are used to derive a variety of other exponents through the use of the scaling relations. Though this latter procedure really provides no additional information, one may reasonably justify some brief indulgence in the former.

Among exponents for which there has been fair agreement in nickel are the measured values of γ and α. Several workers have obtained values for γ in the range 1.30–1.35.[40-44] Some recent measurements of the specific heat of nickel have found α to lie in the range -0.09 to -0.12.[45-47] Using the scaling relation $\alpha + 2\beta + \gamma = 2$ our measured value of β appears to lie at the lower end of the values consistent with these other measurements, although not outside the range permitted by the experimental uncertainties.

Direct calculations of static critical exponents using the renormalization group approach[48] have not yet achieved an accuracy comparable with experiment. At present the most accurate calculations for a Heisenberg ($n = 3$) ferromagnet seem to be provided by high-temperature series expansions. By assuming that the scaling relations may be used to infer the critical behavior below T_C, two recent calculations give $\beta = 0.373 \pm 0.014$,[49] and $\beta = 0.367 \pm 0.020$.[50] Furthermore, scaling theory calculations of the critical amplitudes have given values of B lying in the range 1.22–1.30 for Heisenberg systems.[51,52] The agreement of these calculations to our measured values for nickel is quite satisfactory.

Although such comparisons seem to favor the determination of β made by the zero-field transmission method, the real question of its validity as a useful probe should be addressed more directly. Can such a technique, which manifestly depends on the details of a phenomenologically based theory, really be trusted to the degree implied in our analysis? In particular, can the assumption of a temperature-independent relaxation process really be considered reasonable? The quality of the fit of this theory to the zero-field data suggests that it is. A change in the relaxation time τ of more than about 10% would be extremely noticeable in these curves. The single-crystal data suggest this change is less than 5%. Theoretical calculations of anomalous spin-flip scattering processes of the conduction electrons near a ferromagnetic critical point[19] have suggested the existence of a cusp of $1/\tau$ at T_C. If such a cusp were present in these data it would appear to occur only at reduced temperatures of less than about 10^{-4}.

Thus, this technique seems to provide a useful method for the measurement of the internal magnetization in the absence of any applied field. It has the advantage of acting like a microscopic probe with respect to domain structure while being

unaffected by critical fluctuations.

However, this technique is not without its disadvantages. First of all, it provides useful information only over a limited range of reduced temperature. This could be remedied somewhat by using several frequencies of rf radiation. Higher frequencies would enhance the resonance signal via a longer $\omega\tau$, whereas a lower frequency might allow better resolution nearer the transition temperature. Moreover, a very useful check on this method would be provided by repeating measurements at a second frequency. Such facilities are not, unfortunately, currently at our disposal.

In addition, there are a number of requirements that must be met to apply this technique to a given material. The material must be metallic. It must possess a sufficiently high-saturation magnetization that the resonance peak will occur fairly close to T_C. Most importantly, the relaxation parameter τ must be large compared to $1/\nu_0$, where ν_0 is the frequency of the rf radiation, for the technique to be at all sensitive. Specifically, these conditions require

$$\omega = 2\pi\nu_0 \approx 4\pi M\gamma > 2\pi/\tau,$$

where M refers to the magnetization of the resonance peak and

$$M/M(0) \lesssim 0.5.$$

Thus, we require

$$\gamma M(0) > \nu_0 > 1/\tau.$$

Part of the problem with the earlier work on gadolinium[1,2] was the failure to satisfy this criterion. A measurement of this kind on gadolinium should, however, still be possible at higher frequency. A number of other materials exist for which this technique could reasonably be used at the frequency available. We hope that some of these may be tried in the near future.

Further applied-field measurements are currently being made on our nickel samples. These include some measurements on single crystals as well as extending the polycrystalline measurements to higher temperatures. We hope that these investigations will shed further light on some of the discrepancies noted and that the present theoretical description can be extended to understand some of these interesting details.

Note added in proof. Dewar[53] has pointed out to us that for the polycrystalline zero-field data, the value one obtains for τ in the near peak region depends somewhat more crucially on the guessed value of β than our analysis had suggested. It is preferable, therefore, to obtain τ independently via the applied field measurements on this sample. Using data shown in Figs. 12 and 13, together with the known value of magnetization at the zero-field peak, we obtain $\tau = 2.85\times10^{-10}$ sec $\pm$ 0.15×10^{-10} sec at $T = 325.5$ °C. This gives $\beta = 0.357 \pm 0.012$, a result nearly identical to that stated. β is still obtained most accurately by the single-crystal data analysis, which is correct as given.

ACKNOWLEDGMENTS

We gratefully acknowledge the assistance of Frank C. Chambers and Julia Ju-Wen Tien in some of the lengthy experimental runs. We also thank Patrick C. Gibbons and Stephen E. Schnatterly for many helpful discussions and suggestions.

---

*Research supported by a grant from the NSF DMR 72-03168.

†Present address: Dept. of Physics, University of Illinois, Urbana, Ill. 61801.

[1]P. Sheng, C. N. Manikopoulos, and T. R. Carver, Phys. Rev. Lett. 30, 234 (1973).

[2]C. N. Manikopoulos, P. Sheng, and T. R. Carver, Phys. Rev. B 8, 1131 (1973).

[3]H. E. Stanley, *Introduction to Phase Transitions and Critical Phenomena* (Oxford U.P., Oxford, 1971), p. 185.

[4]K. G. Wilson and J. Kogut, Phys. Rev. C 12, 75 (1974).

[5]M. E. Fisher, Rev. Mod. Phys. 46, 597 (1974).

[6]R. B. Lewis and T. R. Carver, Phys. Rev. Lett. 12, 693 (1964).

[7]R. B. Lewis and T. R. Carver, Phys. Rev. 155, 309 (1967).

[8]For a recent key entry to bibliography, see F. Beuneu and P. Monod, Phys. Rev. B 13, 3424 (1976).

[9]G. C. Alexandrakis, T. R. Carver, and O. Horan, Phys. Rev. B 5, 3472 (1972).

[10]R. M. Bozorth, *Ferromagnetism* (Van Nostrand, New York, 1951), p. 569.

[11]W. J. Carr, Jr., J. Appl. Phys. 29, 436 (1958).

[12]T. L. Gilbert, Phys. Rev. 100, 1234 (1955).

[13]S. M. Bhagat and P. Lubitz, Phys. Rev. B 10, 179 (1974).

[14]H. H. Potter, Proc. R. Phys. Soc. 49, 671 (1937).

[15]S. M. Bhagat and E. P. Chicklis, Phys. Rev. 178, 828 (1969).

[16]See, for example, P. Prutton, *Thin Ferromagnetic Films* (Butterworth, London, 1964).

[17]C. Kittel, Phys. Rev. 70, 965 (1946).

[18]G. C. Alexandrakis, Ph.D. thesis (Princeton University, 1968) (unpublished).

[19]O. Entin-Wohlman, G. Deutscher, and R. Orbach, Phys. Rev. B 11, 219 (1975).

[20]R. B. Lewis, Ph.D. thesis (Princeton University, 1965) (unpublished).

[21]Sauereisen Insalute No. 1, Sauereisen Cement Co., Pittsburgh, Pa. 15238.

[22]Ceramaseal, Inc., New Lebanon Center, N. Y. 12126.

[23]Gasket No. EC-0-SV-13, Emerson and Cuming, Inc., Canton, Mass.
[24]Model S210 Platinum Resistance Thermometer, Minco Products Inc., Minneapolis, Minn. 55432.
[25]J. A. Griffin, Rev. Sci. Instrum. 46, 5 (1975).
[26]Series No. 100 Polishing Jig, Indacom Co., Succasunna, N. J. 07876.
[27]S. J. Rosenberg, *Nickel and Its Alloys*, Natl. Bur. Stds. Monograph No. 106 (U. S. GPO, Washington, D. C., 1968), p. 22.
[28]D. S. Rodbell, Physica 1, 279 (1965).
[29]C. Kittel, *Introduction to Solid State Physics*, 3rd ed. (Wiley, New York, 1968), p. 461.
[30]S. J. Rosenberg, in Ref. 27, p. 25.
[31]Model G-501 NMR Precision Gaussmeter, Harvey-Wells Electronics, Inc., Southbridge, Mass.
[32]N. Bloemberger, Phys. Rev. 78, 572 (1950).
[33]M. B. Salamon, Phys. Rev. 155, 224 (1967).
[34]E. E. Anderson, S. Arajs, A. Stelmach, B. L. Tehan, and Y. D. Yao, Phys. Lett. A36, 173 (1971).
[35]M. Rotter and B. Sedlak, Czech. J. Phys. B 20, 1285 (1970).
[36]H. C. Benski, R. C. Reno, C. Hohenemser, R. Lyons, and C. Abeledo, Phys. Rev. B 6, 4266 (1972).
[37]R. C. Reno and C. Hohenemser, Phys. Rev. Lett. 25, 1007 (1970).
[38]For a discussion of this point, see P. Heller, Rep. Prog. Phys. 30, 731 (1967).
[39]J. L. Oddou, J. Berthier, and P. Peretto, Phys. Lett. A45, 445 (1973).
[40]J. S. Kouvel and M. E. Fisher, Phys. Rev. 136, A1626 (1964).
[41]A. Arrott and J. E. Noakes, Phys. Rev. Lett. 19, 787 (1967).
[42]J. S. Kouvel and J. B. Comly, Phys. Rev. Lett. 20, 1237 (1968).
[43]M. Vicentini-Missoni, R. Joseph, M. Green, and J. L. Sengers, Phys. Rev. B 1, 2312 (1970).
[44]S. Arajs, B. Tehan, E. Anderson, and A. Stelmach, Phys. Status Solidi 41, 639 (1970).
[45]D. L. Connelly, J. S. Loomis, and D. E. Mapother, Phys. Rev. B 3, 924 (1971).
[46]F. L. Lederman, M. B. Salamon, and L. W. Shacklette, Phys. Rev. B 9, 2981 (1973).
[47]J. Major, L. G. Mihaly, and G. Tichy, in Proceedings of the International Conference on Magnetism, Moscow, (unpublished).
[48]The highest-order calculation in the ϵ expansion is presently given by E. Brezin, J-C. Le Guillou, and J. Zinn-Justin, Phys. Rev. B 8, 5330 (1973).
[49]M. Ferer, M. A. Moore, and Michael Wortis, Phys. Rev. B 4, 3954 (1971).
[50]D. S. Ritchie and M. E. Fisher, Phys. Rev. B 5, 2668 (1972).
[51]S. Milosević and H. E. Stanley, Phys. Rev. B 6, 986 (1972).
[52]A. Aharony and P. C. Hohenberg, Phys. Rev. B 7, 3081 (1976).
[53]G. Dewar (private communication).